MAJOR ARTICLE

Distribution of Cell-Free and Cell-Associated HIV Surrogates in the Female Genital Tract After Simulated Vaginal Intercourse

Nicolette A. Louissaint, Edward J. Fuchs, Rahul P. Bakshi, Sridhar Nimmagadda, Yong Du, Katarzyna J. Macura, Karen E. King, Richard Wahl, Arthur J. Goldsmith, Brian Caffo, Ying Jun Cao, Jean Anderson, and Craig W. Hendrix

Background. Rational development of drugs to prevent human immunodeficiency virus (HIV) transmission benefits from an understanding HIV distribution in the female genital tract after intercourse. This study describes HIV distribution using surrogates of cell-free and cell-associated HIV and semen.

Methods. Apheresis-derived, autologous, lymphocyte-rich cells radiolabeled with 3.7-MBq (100-μCi) indium 111 (^{111}In)–oxine (cell-associated HIV surrogate) and 18.5-MBq (500-μCi) technetium 99m (^{99m}Tc)–sulfur colloid (HIV-sized 100-nm particle, cell-free HIV surrogate) were resuspended in 3 mL of hydroxyethylcellulose gel (semen simulant) with gadoteridol and dosed via artificial phallus after simulated intercourse. Postdosing dual-isotope single photon emission computed tomography with computed tomography (SPECT/CT) and magnetic resonance (MR) images were acquired to determine the surrogates' distribution. Seven hours after dosing, vaginal biopsy and luminal samples were collected at discrete locations in 8 subjects.

Results. SPECT/CT and MR analysis showed HIV and semen surrogate distribution with highest signal intensity in the vaginal pericervical area, without detectable signal in the uterus. One-third of the administered dose was retained in the female genital tract after 4 hours. Cell-free and cell-associated surrogate distribution coincided.

Conclusions. We demonstrate the feasibility of dual-isotope SPECT/CT and MR imaging to determine the distribution of HIV and semen surrogates after simulated intercourse without disrupting vaginal contents. Surrogate distribution suggests topical microbicides do not need to reach the uterus for efficacy.

The design of effective vaginal microbicides benefits from an understanding of distribution and clearance of human immunodeficiency virus (HIV) among sites of exposure within the female genital tract, including luminal and mucosal distribution after ejaculation of HIV-infected semen [1–5]. Details of HIV infection have not been determined in humans but are essential for rational design of microbicide candidates to outdistance and outlast HIV after intercourse.

Previous investigators used noninvasive imaging with indium 111 (^{111}In)–labeled leukocytes to observe in vivo leukocyte migration for anatomic localization of infection and inflammation [6–11]. We have used serial single-photon emission computed tomography with computed tomography (SPECT/CT) to describe HIV surrogate distribution and clearance in the distal part of the colon [12]. Other groups have used gamma scintigraphy and/or magnetic resonance (MR) imaging to image distribution of gels and fluid in the female genital tract [13–20], sometimes with simulated receptive vaginal intercourse. In these studies, vaginal distribution was evaluated within 1 hour of dosing. Although MR imaging has been a useful tool for assessing fluid and gel distribution in the female genital tract [14, 15, 18, 21, 22], it is limited in its ability to quantitatively and simultaneously detect multiple chemical markers. To circumvent these limitations, we used radiolabeled cell-free and cell-associated HIV surrogates, with different isotope emission energies, mixed with a semen surrogate labeled with gadolinium. We then simulated intercourse to assess HIV surrogate distribution within the female genital tract.

Received 18 May 2011; accepted 27 September 2011; electronically published 25 January 2012.

Correspondence: Craig W. Hendrix, MD, Harvey 502, 600 N Wolfe St, Baltimore, MD 21287 (chendrix@jhmi.edu).

The Journal of Infectious Diseases 2012;205:725–32

DOI: 10.1093/infdis/jir841

METHODS

Research Participants

The study protocol was approved by the Johns Hopkins Medicine Institutional Review Board. All subjects provided informed consent. Eligible subjects were premenopausal women aged ≥21 years who had comfort with vaginal dilatory objects, a negative pregnancy test, intact uterus, lymphocyte counts within normal limits, neutrophil count ≥1000 cells/mm^3, platelet counts ≥150 000 cells/mm^3, and prothrombin time/partial thromboplastin time results within normal limits.

Study Schema

Once subjects passed screening, a surrogate for HIV-infected ejaculate was prepared from apheresis-derived, autologous, radiolabeled lymphocyte-rich cells and radiolabeled HIV-sized particles mixed in semen simulant. Radiolabeled simulated ejaculate was injected into the vagina through the lumen of an artificial phallus after simulated receptive vaginal intercourse. SPECT/CT and MR images and cervicovaginal lavage (CVL), vaginal wall and forniceal biopsy, and luminal brush samples were collected during the next 8 hours to assess distribution of radiolabeled HIV surrogates.

HIV Surrogate Dose Preparation

Each subject underwent apheresis for 2 hours, during which lymphocyte-enriched leukocytes were isolated from whole blood via peripheral access. The cell-associated HIV surrogate was created by labeling apheresis-derived autologous leukocytes with ^{111}In-oxine (Cardinal Health). The cell-free HIV surrogate, technetium 99m (^{99m}Tc)–sulfur colloid (SC), consisted of 100-nm radiolabeled particles. The final dose was 3.7-MBq (100-μCi) ^{111}In-labeled leukocytes, 18.5-MBq (50-μCi) ^{99m}Tc-SC, and 1:100 gadolinium. (Gadolinium was used only in the last 5 of 8 subjects.) These components were resuspended in 3 mL of hydroxyethylcellulose (HEC) gel (Pre-Seed; INGfertility), our iso-osmolar semen surrogate, at dosing.

Coital Simulation

This study used a simulated receptive vaginal intercourse model, similar to a previously developed model that simulates coital forces for receptive anal intercourse [12]. We used a coital dynamic simulator (CDS) (an artificial phallus with an intravenous catheter in the urethral position) to simulate coital forces of receptive vaginal intercourse and permit dosing of the simulated ejaculate. This CDS was inserted and manipulated for 5 minutes, 1 cycle/second to simulate receptive vaginal intercourse (metronome guided). To simulate ejaculation, the CDS remained fully inserted into the vagina, and the investigator injected the radiolabeled dose through the lumens in the CDS with catheter dead-space flush. The subject then manipulated the CDS for 10 more cycles before removing the device. The retained dose was estimated by subtracting the residual radioactivity for both radiolabels in all devices after dosing using a dose calibrator (CRC 15-W; Capintec).

SPECT/CT Imaging

SPECT/CT images were acquired at 0–1 and 3–4 hours after dosing. Fusion of SPECT and CT images produces an image with SPECT signal intensity within a CT-defined anatomic location [10]. SPECT/CT images of radiotracers were acquired using a dual-head VG series system (GE Medical Systems) equipped with a low-dose CT unit (Hawkeye). CT images were acquired before SPECT images. CT scans (1-cm thickness; step-and-shoot mode; 140 kVp; 1.0 mA; 180° fan angle) were acquired from the thorax to the anus over a 213° arc. CT images were reconstructed with filtered back-projection onto a 256 × 256-matrix. Noise correction was performed using automatic body contouring to optimize signal and resolution. Simultaneous dual-isotope image acquisition was performed with a 20% ^{99m}Tc energy window centered at 140 keV and 20% ^{111}In energy windows centered at 172 and 247 keV. Projections from 2 ^{111}In energy windows were added together to reduce noise. Each SPECT acquisition was 35 minutes. The SPECT images were then reconstructed into a 128 × 128-matrix size using an iterative ordered subset–expectation maximization (OSEM) algorithm [23].

The downscatter from ^{111}In into the ^{99m}Tc energy window was estimated and compensated for using a model-based method [24]. In this method, object scatter was modeled using the effective-source scatter estimate technique, including contributions from both ^{111}In photon peaks [25]. Photon interactions inside the collimator-detector system, including penetration and scatter components, were estimated using precomputed tables calculated from Monte Carlo simulations. Estimated downscatter was compensated for during iterative OSEM reconstruction of the ^{99m}Tc images by adding the downscatter estimate to the computed projections at each iteration. SPECT images were also compensated for attenuation, scatter, and detector resolution blur during reconstruction [26].

To assess the anatomic distribution of cell-free (^{99m}Tc) relative to the cell-associated (^{111}In) HIV surrogates, we described a mass-adjusted volume of distribution coincident to both isotopes and the volume unique to each isotope, using corrected values filtered by a threshold gating 5% of the total acquired signal for analysis. The percent coincidence of each isotope was calculated to determine the amount of overlap in distribution of the viral surrogates, using disintegrations per minute (dpm), as follows:

% ^{111}In overlap with ^{99m}Tc = Σ (^{111}In dpm within ^{99m}Tc distribution)/Σ (^{111}In dpm total)

and

% ^{99m}Tc overlap with ^{111}In = Σ (^{99m}Tc dpm within ^{111}In distribution)/Σ (^{99m}Tc dpm total).

MR Imaging

MR images were acquired at 1–2 and 4–5 hours after dosing. Images were acquired using a 3.0-T whole-body TRIO imager (Siemens Medical Solutions USA) using the Total Image Matrix body matrix coil (Siemens Medical Solutions USA). Participants were imaged in the supine position. The following sequences were obtained: (1) sagittal, T2-weighted images with fat suppression (7470/160 [repetition time (TR) ms/echo time (TE) ms]; section thickness, 3 mm; intersection gap, 0.9 mm); (2) axial, T2-weighted turbo spin-echo images (9670/116; section thickness, 3 mm; intersection gap, 0.9 mm); and (3) 3-dimensional T1-weighted gradient-echo images with fat suppression (8.8/3.2; section thickness, 2 mm; intersection gap, 0 mm; flip angle, 10°).

MR images were analyzed to assess fluid and semen surrogate distribution in the female genital tract with contrast enhancement using 1:100 gadolinium-containing gadoteridol injection solution (molecular weight, 559 g/mol; 630 mOsm/Kg: pH 6.5–8.0) (ProHance; Bracco Diagnostics) [11–13]. Three-dimensional T1-weighted gradient-echo MR images were reconstructed into axial, coronal, and sagittal images for contrast distribution analysis.

Vaginal Sampling

Between 7 and 8 hours after dosing, a speculum was inserted into the vagina, and 8 cytologic brush samples were collected at the endocervix (n = 2), ectocervix (n = 2), posterior fornix (n = 1), anterior fornix (n = 1), and vaginal wall (n = 2). For the CVL, 10 mL Normosol-R (Hospira) was applied against the cervix, and the lavage fluid was collected into a syringe with Luer Lock tip. For the first 3 subjects, 2 vaginal wall biopsy samples were collected. For the last 5 subjects, biopsy samples were taken from adjacent positions on the vaginal wall (n = 2) and posterior fornix (n = 3).

Vaginal Tissue Cell Extraction and Subset Isolation

To release cells, tissue biopsies were incubated with a dissociative enzyme cocktail of collagenase (0.5 mg/mL; Sigma-Aldrich), DNase (2 U; Roche), elastase (12 U; Worthington Biochemicals), and hyaluronidase (60 U; Worthington Biochemicals). The digestions were carried out in Roswell Park Memorial Institute medium with 7.5% fetal bovine serum in 50-mL conical tubes at 37°C with agitation (Invitrogen). The cells freed from the matrix were isolated by filtration with a 70-μm cell strainer and centrifugation at 400 *g* for 10 minutes at 4°C. Cells were counted using the Guava/Millipore EasyCyte Plus system (Millipore). $CD4^+$ cells were isolated via positive selection with CD4 microbeads using magnetic affinity column separation from a 100-μL aliquot of the administered dose and from tissue-extracted cells (Miltenyi). $CD4^+$ and $CD4^-$ fractions were assessed for radioactivity, cell counting, and flow-cytometric analysis. The dosed ^{111}In-labeled leukocyte radioactivity was used to calculate the number of exogenously administered cells present in the tissue fraction using the following equation: $dpm_{tissue}/(dpm/cell)_{dose}$.

Measurement of Radioactivity

Radioactivity in the biopsy or brush sample was measured on a gamma spectrometer using 2 energy levels (Perkin Elmer). The ^{99m}Tc counts were determined in the 99–150-keV window, with the peak at detected 140 keV (±10 keV); ^{111}In counts were quantified in the 150–500-keV energy window, with peaks detected at 172 and 247 keV (±10 keV). Calculations were corrected for crosstalk, background, and decay.

Statistics

Data were summarized using medians and interquartile ranges (IQRs). The Wilcoxon matched-pairs signed rank test was used to test comparisons, with differences defined as statistically significant at $P \leq .05$.

RESULTS

Subjects

Eight premenopausal women, 21–45 years of age, completed the study. Six of the women were African American, and 2 were white. Two of the subjects were HIV positive. Six women were studied during the luteal phase of their menstrual cycles, and 2 during the follicular phase.

SPECT/CT Distribution of Viral Surrogates

The median dose retained in the subjects was 3.89 MBq for ^{99m}Tc-SC (IQR, 1.67–5.33 MBq) and 3.52 MBq for ^{111}In-labeled cells (IQR, 3.48–3.55 MBq). The median number of cells retained was 2.2 million (IQR, 1.6–4.2 million), about twice the upper limit of typical semen leukocytes. Visual inspection of SPECT/CT images showed distribution of cell-free and cell-associated HIV surrogates in the vaginal lumen with no detectable uterine distribution (Figure 1). SPECT/CT showed the highest signal intensity in the pericervical area (cervical os and fornices) for all subjects. Signal intensity was greatly diminished, if not below detection limits, in the midvaginal position in all subjects. Comparisons of 1- and 3-hour SPECT/CT acquisitions disclosed no change in distribution, although signal intensity decreased. Compared with the scan immediately after dosing (100% reference), subjects retained a median of 55% (IQR, 44%–68%) of ^{111}In and 31% (IQR, 24%–44%) of ^{99m}Tc signals at SPECT/CT 3 hours after dosing.

The distribution of both radiolabels seemed to be largely coincident on visual inspection of the maximal-intensity

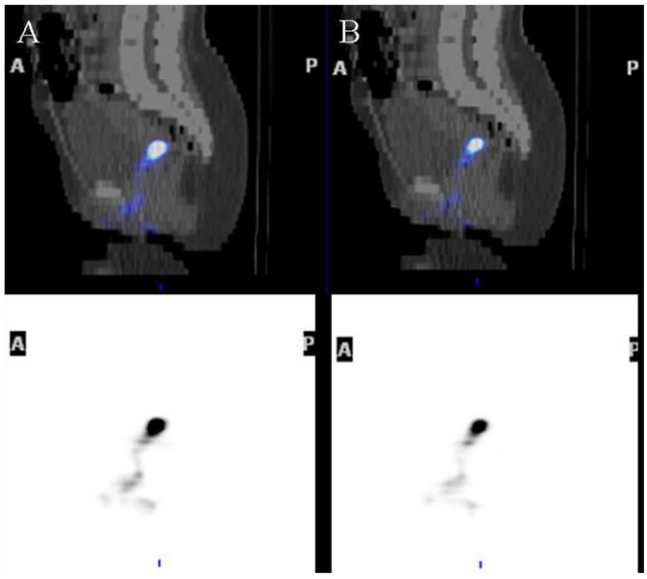

Figure 1. Single photon emission computed tomography with computed tomography (SPECT/CT) distribution of human immunodeficiency virus (HIV) surrogates after simulated vaginal intercourse. SPECT/CT fusion image shows the distribution of radioactivity in the indium 111 window (*A*) (cell-associated HIV surrogate) and technetium 99m window (*B*) (cell-free HIV surrogate) after 1 h. The anatomic distributions of both surrogates at SPECT are similar, and endometrial distribution is not evident. Bottom images are maximal intensity projections; top images, center-section sagittal images.

projection figures for all subjects (Figure 1). The median percentage of ^{99m}Tc signal that overlapped with the ^{111}In signal was 94% (IQR, 86%–97%) 1 hour after dosing and lower, 78% (IQR, 62%–84%), 3 hours after dosing ($P < .01$). The median percentage of ^{111}In signal that overlapped with the ^{99m}Tc signal was 82% (IQR, 67%–83%) 1 hour after dosing and lower, 58% (IQR, 51%–65%), 3 hours after dosing ($P < .01$).

MR Imaging Distribution of Semen Simulant

The T1-weighted MR images showed gadolinium distributed throughout the vagina, with no detectable uterine distribution (Figure 2). The distribution of gadolinium showed similar signal intensity throughout the entire vagina, with evident forniceal pooling. The signal intensity throughout the endometrial canal was consistent with endometrial tissue, not gadolinium, based on comparison of T2-weighted and T1-weighted images.

Direct Assessment of Vaginal Distribution

Moving from distal to proximal (left to right in Figure 3*C*), the direct brush sampling showed increasing radiolabel, with peak activity at the fornices or cervical os in all subjects seen with both isotopes. The signal activity at the midvaginal position had a median of 0.04% (IQR, 0.03%–0.09%) of the ^{111}In dosed and 0.15% (IQR, 0.08%–0.39%) of the ^{99m}Tc dosed. In comparison, the signal increased to a median of 0.31% (IQR, 0.07%–0.85%) of the ^{111}In dosed and 1.79% (IQR, 0.44%–1.48%) of the ^{99m}Tc dosed at the peak pericervical location (both $P < .01$). Qualitatively, the pattern of the 1- and 3-hour SPECT radiolabel (sequential axial section signal intensity) corresponded with measurements from discrete anatomic sites via brush sampling (Figure 4).

Total and CD4$^+$ cell yields did not differ between vaginal wall and forniceal biopsy samples; results from all biopsies in each woman were pooled. Median cell yield/biopsy from each subject was 328 815 (IQR, 256 149–938 740), of which 6% (IQR, 6%–10%) were CD4$^+$ cells. We estimated that 0.08% (IQR, 0.03%–0.058%) of total cells and 0.12% (0.04%–0.76%) of CD4$^+$ cells were from the radiolabeled dose. ^{99m}Tc was also associated with the cells, with a median of 8111 dpm (IQR, 345–16 905 dpm) or 0.0004% of the initial dose associated with the cellular fraction in each biopsy sample.

Analysis of CVL samples obtained 7–8 hours after the initial dose (after brush sampling and before biopsies) found medians of 0.95% (IQR, 0.89%–1.2%) and 3.15% (IQR, 1.62%–4.40%) of the original retained dose of cell-associated (^{111}In) and cell-free (^{99m}Tc) HIV surrogates, respectively. We did not identify any differences in the results described above based on menstrual phase or HIV status. The sample size was too small to exclude anything but large differences in our quantitative measures.

DISCUSSION

This study evaluated the feasibility of using noninvasive imaging of HIV surrogates to describe HIV distribution in the female genital tract after receptive vaginal intercourse. Radioactive labeling of the HIV surrogates permits SPECT/CT imaging to determine the distribution of each radiotracer independently. Simultaneous dosing of simulated semen (gadolinium-labeled HEC gel) with HIV surrogates (^{99m}Tc-SC and ^{111}In leukocytes) enables the use of both MR imaging and SPECT/CT to analyze semen and HIV surrogate distribution. This noninvasive imaging method enables quantitative assessments of HIV surrogate distribution in the vagina after coitus, without disrupting the distribution of contents within the lumen of the vagina with invasive sampling methods. This also allows repeated assessments over time, which would be limited primarily by radiolabel half-life.

Coincidental distribution analysis using SPECT revealed vaginal distribution of both HIV surrogates, which were most often characterized by pericervical and forniceal pooling. There was no detectable intrauterine distribution. Similarly, MR imaging using a 559-g/mol–molecular weight

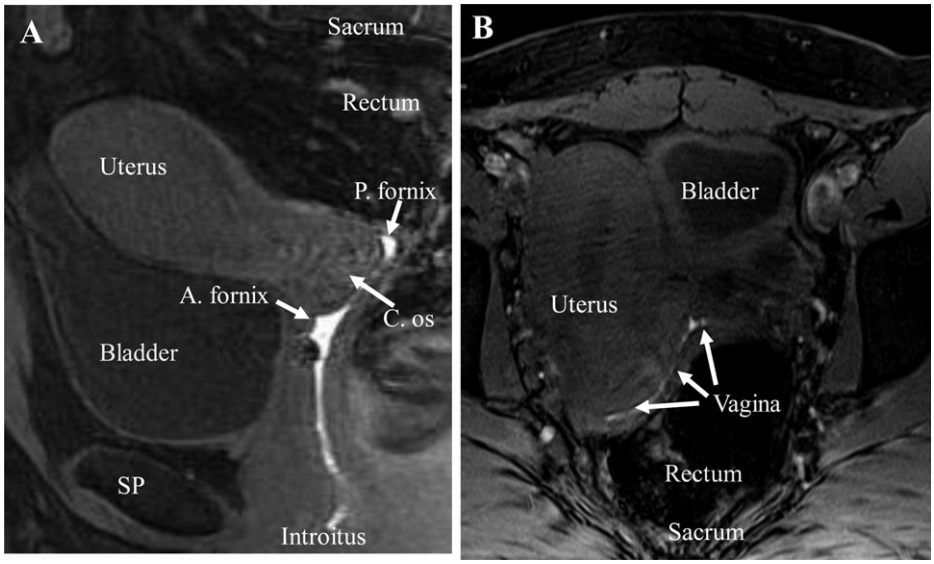

Figure 2. Magnetic resonance imaging (T1-weighted) detection of female genital tract anatomy and gadolinium-labeled hydroxyethylcellulose gel distribution in the sagittal (*A*) and transaxial (*B*) views, 2 hours after dosing in a representative subject. A. fornix, anterior fornix; C. os, cervical os; P. fornix, posterior fornix; SP, symphysis pubis.

gadolinium-labeled molecule did not show any intrauterine distribution on MR images. All dosed moieties were detectable by imaging up to 4–5 hours after dosing, the time of the last imaging studies. These findings also revealed that distribution of both surrogates was practically identical in the initial period after dosing but appeared to diverge somewhat at later time points. The reason for this divergence is unclear; it may result from differences in surrogate affinity for mucosal constituents or colloidal characteristics. This divergence needs to be confirmed with HIV particles in place of our surrogate. For now, the divergence of the HIV surrogates over time suggests that future microbicide distribution studies may need to be performed coincidently with the most widely distributed HIV surrogate in order to capture the widest distribution possible. It remains, however, for us to validate the HEC semen simulant distribution in direct comparison with human semen. Important differences include lower viscosity of human semen after liquefaction and the presence of seminal prostaglandins, which affect uterine contractility.

It was anticipated that the signal associated with our HIV surrogates would be detected in the uterine cavity, based on findings of previous studies using ^{99m}Tc-labeled human albumin microspheres (reported to be similar in size to spermatozoa) that showed radiolabel distribution in the uterus, fallopian tubes, and peritoneal space after deposition into the vaginal fornices [17, 19, 20]. These studies, which employed human albumin microspheres, used an uncertain delivery vehicle and prolonged maintenance of the supine position. In contrast, there are also numerous other studies of vaginally dosed gels using imaging of small molecules (typically diethylenetriaminepentaacetic acid [DTPA]) with gamma scintigraphy or MR imaging that consistently demonstrate no uterine distribution [14–16, 22, 27, 28]. Subjects in our study, and most of the other studies without uterine distribution, had many of these factors in common, in contrast to the microsphere studies. For example, most of the studies without uterine distribution used lower radiation doses and allowed ambulation after early imaging, which is associated with increased proximal distribution [28, 29] and may result in increased loss of signal from the vagina.

The polymer gel vehicles used in most of the nonuterine distribution studies may have different release characteristics that slowed or inhibited radiolabeled molecule release. Many of these studies used small-molecule radiolabels (^{99m}Tc-DTPA [molecular weight, 492 g/mol], In-DTPA [504 g/mol], Gd-DTPA [590 g/mol], gadoteridol [559 g/mol), and we used 100-nm SC particles; all are well below the spermatozoa-sized microsphere molecule. The exception to smaller-molecule radiolabels in studies showing no uterine distribution studies is our radiolabeled lymphocytes, which are much larger than microspheres. Uterine peristaltic activity may explain the rapid microsphere migration; this peristalsis may be sensitive to specific molecular triggers that differ among radiolabels used. It is unclear which of these factors (specific-size sieving, stimuli to peristaltic activity, loss of radiolabel, lower radiation dose, and delivery vehicle chemistry) contributed to differences in uterine distribution. Future researchers would be well advised to take account of potentially influential physiologic variation, including differences in cervical mucus,

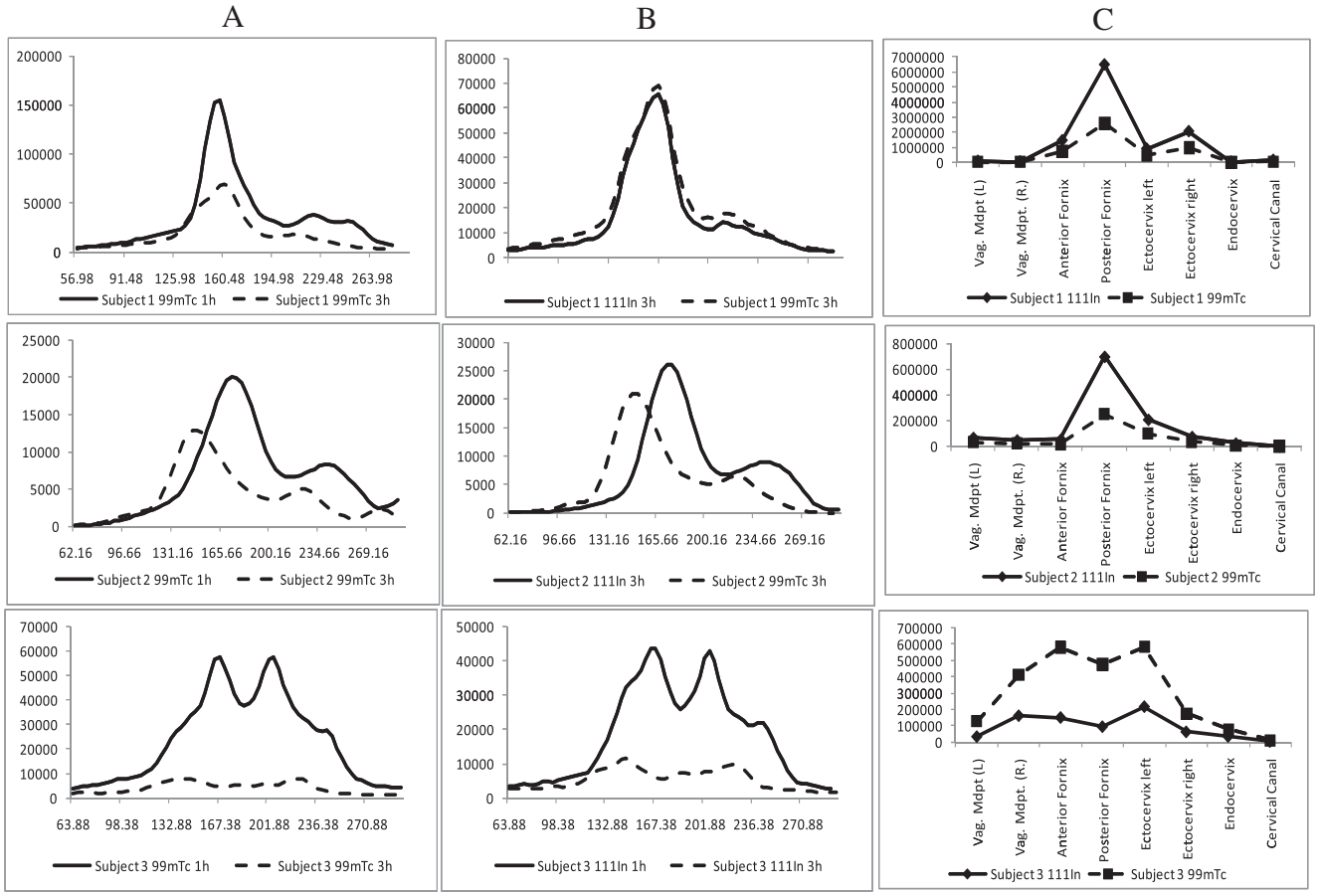

Figure 3. Correlation between radioactivity detected by direct sampling with endoscopic brushes and single photon emission computed tomography with computed tomography (SPECT/CT) in 3 representative subjects. *A, B,* Distribution of radioactivity at 1-h (*A*) and 3-h (*B*) SPECT/CT. *C,* Radioactivity distribution as measured by cytobrush sampling 7 hours at dosing.

which varies with menstrual phase, and the effects of seminal prostaglandins on uterine contractility. Whatever the cause, even if our method was insensitive to uterine distribution, the relative uterine distribution was many orders of magnitude lower than the dose delivered to the pericervical area, given the precipitous drop in concentration from the highest concentration at the cervical os and fornices to an unmeasured signal below detection limits in the endometrial cavity.

Confirmation of the absence of uterine distribution of HIV surrogates is critical, because it implies that vaginal gels, films, or drug-eluting rings, whose active ingredients distribute to intravaginal locations alone, may be adequate. Direct sampling of the endometrial cavity with sheathed brushes may help determine whether any radioactivity is present within the uterus. However, the potential for radioactive contamination of the sheathed brush during passage through the "hot" pericervical area may not achieve a clear result. More physiologic postcoital conditions, possibly including fresh ejaculate with motile spermatozoa and seminal plasma, are needed to finally rule out uterine distribution of HIV-sized particles deposited along with ejaculate.

Although noninvasive imaging is a useful tool to measure distribution, direct sampling is helpful to determine the concentration of HIV surrogates or drug concentration at specific sites within the tissue, in contrast to more continuous SPECT/CT and MR imaging. The amount of radioactivity associated with the tissue biopsy samples, and the cells extracted from the tissue matrix, reveals that both surrogates associate with the tissue (and tissue cells) for up to 8 hours after dosing. HIV surrogates may simply be trapped superficially on the mucosal surface or may have migrated within the epithelial cell layer and/or mucosal tissue. Resolving this question requires further methodologic development. The association of both HIV surrogates with tissue biopsy samples, seen in vaginal tissue after vaginal exposure here and in rectal tissue after rectal exposure in another study, suggests that both forms of HIV may be relevant sources of HIV transmission in both the female genital tract and the distal colon [30].

A key concern with local sampling is the impact of sampling instrumentation on HIV surrogate distribution through either distortion of distribution or contamination of the radiolabel

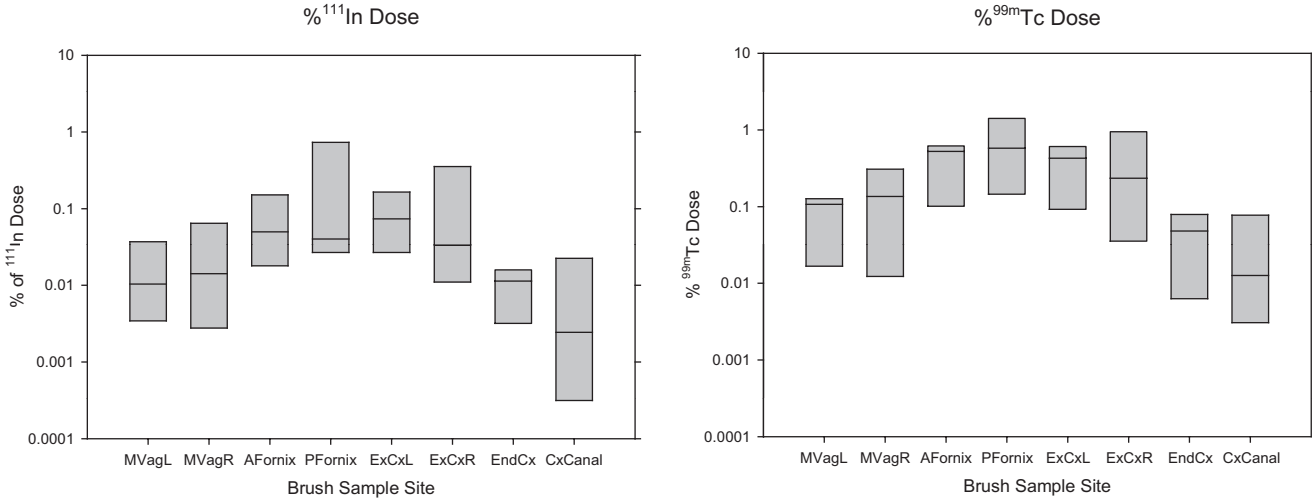

Figure 4. Luminal radioactivity at each anatomic location measured after direct sampling with cytobrushes. *A,* Indium 111 (^{111}In) radioactivity at each site relative to total dose. *B,* Technetium 99m (^{99m}Tc) radioactivity at each site relative to total dose.

from one area of the female genital tract to another. Samples were collected from the vagina moving toward the cervix, the site of greatest signal intensity, to minimize contamination of low-signal areas with areas of high signal. Because the cytobrush was placed in the vagina unsheathed, contamination from other sites was possible, especially for the cervical canal samples. The insertion of the vaginal speculum and the collection of a large-volume CVL sample are factors that would have altered natural distribution. However, only biopsy samples were obtained after the CVL, so the expected impact of the CVL on the tissue measurements is small. Finally, the qualitative correlation of direct sampling and imaging results suggests that the impact of sampling methods on distribution was insignificant.

The limitations of our study design and methods suggest that several future studies are needed to better validate or explain our findings. These studies include (1) validation of cell-free HIV distribution, comparing our surrogate and autologous HIV in infected individuals; (2) validation of the HEC semen surrogate by comparison with partner ejaculate, using HIV-radiolabeled surrogates; and (3) combined autoradiographic and histologic analysis of tissue biopsy samples after simulated HIV exposure to confirm that our finding of radiolabeled tissue samples actually represents HIV surrogates beyond the surface or epithelial layer of the tissue.

We demonstrated the feasibility of assessing the distribution and migration of HIV surrogates within the female genital tract by using complementary indirect imaging and direct sampling methods as a first step toward understanding the distribution of HIV after receptive vaginal intercourse. Validation against more physiologic postcoital conditions remains to be done. This is especially important for establishing whether or not vaginal microbicides need to be distributed into the uterine cavity to outdistance and outlast HIV.

Notes

Acknowledgments. We are grateful for the contributions of our volunteers and to the clinical staff of the Drug Development Unit, especially Stephanie Everts, the laboratory staff of the Clinical Pharmacology Analytical Laboratory within the Division of Clinical Pharmacology, and David Clough and Jeff Leal in the Department of Radiology.

Financial support. This work was supported by funding from the US Agency for International Development (contract GPOA 0005004100) through the International Partnership for Microbicides.

Potential conflicts of interest. All authors: No reported conflicts.

All authors have submitted the ICMJE Form for Disclosure of Potential Conflicts of Interest. Conflicts that the editors consider relevant to the content of the manuscript have been disclosed.

References

1. Bentley ME, Fullem AM, Tolley EE, et al. Acceptability of a microbicide among women and their partners in a 4-country phase I trial. Am J Public Health **2004**; 94:1159–64.
2. Ramjee G, Morar NS, Alary M, et al. Challenges in the conduct of vaginal microbicide effectiveness trials in the developing world. AIDS **2000**; 14:2553–7.
3. Foss AM, Watts CH, Vickerman P, Heise L. Condoms and prevention of HIV. BMJ **2004**; 329:185–6.
4. Hladik F, Hope TJ. HIV infection of the genital mucosa in women. Curr HIV/AIDS Rep **2009**; 6:20–8.
5. De Clercq E. HIV-chemotherapy and -prophylaxis: new drugs, leads and approaches. Int J Biochem Cell Biol **2004**; 36:1800–22.
6. Signore A, Sensi M, Pozzilli C, Negri M, Lenzi G, Pozzilli P. Effect of unlabeled indium oxine and indium tropolone on the function of isolated human lymphocytes. J Nucl Med **1985**; 26:4.
7. Issekutz T, Chin W, Hay J. Measurement of lymphocyte traffic with indium-111. Clin Exp Immunol **1980**; 39:7.
8. Silberstein E, Watson S, Mayfield G, Kereiakes J, Bullock W. Indium 111 toxicity in the human lymphocyte. J Lab Clin Med **1985**; 105:5.

9. ten Berge R, Natarajan A, Hardeman M, van Royen E, Schellekens P. Labeling with indium-111 has detrimental effects on human lymphocytes: concise communication. J Nucl Med **1983**; 24:6.
10. Puncher MR, Blower PJ. Frozen section microautoradiography in the study of radionuclide targeting: application to indium-111-oxine-labeled leukocytes. J Nucl Med **1995**; 36:7.
11. Chen JJ, Huang JC, Shirtliff M, et al. CD4 lymphocytes in the blood of HIV^+ individuals migrate rapidly to lymph nodes and bone marrow: support for homing theory of CD4 cell depletion. J Leukoc Biol **2002**; 72:8.
12. Hendrix CW, Fuchs EJ, Macura KJ, et al. Quantitative imaging and sigmoidoscopy to assess distribution of rectal microbicide surrogates. Clin Pharmacol Ther **2008**; 83:97–105.
13. Abcarian H, Gant NF, Grant RE, Lewis FR Jr, Gardner TJ. Ten specialty boards report accomplishments and plans: part II. Bull Am Coll Surg **2004**; 89:40–59.
14. Barnhart KT, Pretorius ES, Timbers K, Shera D, Shabbout M, Malamud D. In vivo distribution of a vaginal gel: MRI evaluation of the effects of gel volume, time and simulated intercourse. Contraception **2004**; 70:498–505.
15. Barnhart KT, Pretorius ES, Timbers K, Shera D, Shabbout M, Malamud D. Distribution of a 3.5-mL (1.0%) C31G vaginal gel using magnetic resonance imaging. Contraception **2005**; 71:357–61.
16. Brown J, Hooper G, Kenyon CJ, et al. Spreading and retention of vaginal formulations in post-menopausal women as assessed by gamma scintigraphy. Pharm Res **1997**; 14:1073–8.
17. Kunz G, Beil D, Deininger H, Wildt L, Leyendecker G. The dynamics of rapid sperm transport through the female genital tract: evidence from vaginal sonography of uterine peristalsis and hysterosalpingoscintigraphy. Hum Reprod **1996**; 11:627–32.
18. Pretorius ES, Timbers K, Malamud D, Barnhart K. Magnetic resonance imaging to determine the distribution of a vaginal gel: before, during, and after both simulated and real intercourse. Contraception **2002**; 66:443–51.
19. Venter PF, Iturralde M. Migration of a particulate radioactive tracer from the vagina to the peritoneal cavity and ovaries. S Afr Med J **1979**; 55:917–19.
20. Zervomanolakis I, Ott HW, Hadziomerovic D, et al. Physiology of upward transport in the human female genital tract. Ann N Y Acad Sci **2007**; 1101:1–20.
21. Barnhart K, Pretorius ES, Stolpen A, Malamud D. Distribution of topical medication in the human vagina as imaged by magnetic resonance imaging. Fertil Steril **2001**; 76:189–95.
22. Barnhart KT, Pretorius ES, Shaunik A, Timbers K, Nasution M, Mauck C. Vaginal distribution of two volumes of the novel microbicide gel cellulose sulfate (2.5 and 3.5 mL). Contraception **2005**; 72:65–70.
23. Hudson HM, Larkin RS. Accelerated image reconstruction using ordered subsets of projection data. IEEE Trans Med Imaging **1994**; 13:601–9.
24. Du Y, Frey E. Model-based downscatter compensation for simultaneous Tc-99m/In-111 dual-isotope SPECT imaging; J Nucl Med. Meeting Abstracts, May **2008**; 49:152P.
25. Frey EC, Tsui B. A new method for modeling the spatially-variant, object-dependent scatter response function in SPECT. In: Conference Record of the Nuclear Science Symposium. Anaheim, CA, **1996**; 1082–6.
26. Du Y, Tsui BM, Frey EC. Model-based crosstalk compensation for simultaneous 99mTc/123I dual-isotope brain SPECT imaging. Med Phys **2007**; 34:3530–43.
27. Chatterton BE, Penglis S, Kovacs JC, Presnell B, Hunt B. Retention and distribution of two 99mTc-DTPA labelled vaginal dosage forms. Int J Pharm **2004**; 271:137–43.
28. Mauck CK, Katz D, Sandefer EP, et al. Vaginal distribution of Replens and K-Y Jelly using three imaging techniques. Contraception **2008**; 77:195–204.
29. Menon S, Izquierdo A, Rosen M, Hummel A, Barnhart K. The effect of ambulation on vaginal distribution of miconazole nitrate (1200 mg). J Womens Health (Larchmt) **2007**; 16:703–6.
30. Miller CJ, Shattock RJ. Target cells in vaginal HIV transmission. Microbes Infect **2003**; 5:59–67.